Improved repeatability of subsolid nodule measurement in low-dose lung screening with monoenergetic images: a phantom study

Jihang Kim, Kyung Hee Lee, Junghoon Kim, Yoon Joo Shin, Kyung Won Lee

Department of Radiology, Seoul National University Bundang Hospital, Gyeonggi-do, Korea

Correspondence to: Kyung Won Lee. Department of Radiology, Seoul National University Bundang Hospital, 82, Gumi-ro 173beon-gil, Bundang-gu, Seongnam-si, Gyeonggi-do 13620, Korea. Email: lkwrad@gmail.com.

Background: To investigate whether monoenergetic images captured with dual-layer spectral computed tomography (CT) can improve the repeatability of subsolid nodule measurement, and whether this approach can further reduce the radiation dose of CT while maintaining its measurement repeatability.

Methods: An anthropomorphic phantom with simulated subsolid nodules at three different levels was repeatedly scanned with both conventional single-energy CT and dual-layer spectral CT. A proxy for the measurement repeatability in the National Lung Screening Trial (proxy for NLST) was calculated with the typical CT protocol used in NLST. Using the dual-layer spectral CT, monoenergetic images of 40 to 110 keV, with an interval of 10 keV, were generated. The average diameter and volume of a total of 15,120 nodules in 840 CT images were measured by using a commercially-available computer-aided detection (CAD) system. The repeatability coefficient (RC), %RC, and 95% confidence intervals (CIs) of each image set were calculated and compared.

Results: At the same tube voltage and tube current-time product, monoenergetic images resulted in significantly lower RC than the proxy for NLST, indicating that measurement repeatability was enhanced. When the radiation dose was lowered by 30% or 55%, monoenergetic images showed significantly lower RC at high-energy keV than the proxy for NLST. The estimated measurement repeatability from monoenergetic images with 30% or 55% lower radiation dose was comparable to the repeatability from conventional single-energy CT images with standard radiation dose and iterative reconstruction.

Conclusions: Monoenergetic images captured by using dual-layer spectral CT can improve the repeatability of subsolid nodule measurement. The use of monoenergetic images would allow lung cancer screening with a lower radiation dose, while maintaining comparable measurement repeatability.

Keywords: Dual-layer spectral CT; lung cancer screening; measurement repeatability; monoenergetic image; radiation dose

Introduction

The National Lung Screening Trial (NLST) showed that the use of low-dose computed tomography (CT) for screening in a high-risk population reduces mortality from lung cancer (1). Lung cancer screening guidelines require a variety of management approaches, according to the size

and size changes of the nodules (2,3). Thus, in addition to nodule detectability, measurement repeatability is an essential factor in screening CT for follow-up and risk assessment of pulmonary nodules. Because annual CT screening increases the risk of radiation-related cancers (4), it is also important to minimize the radiation dose during
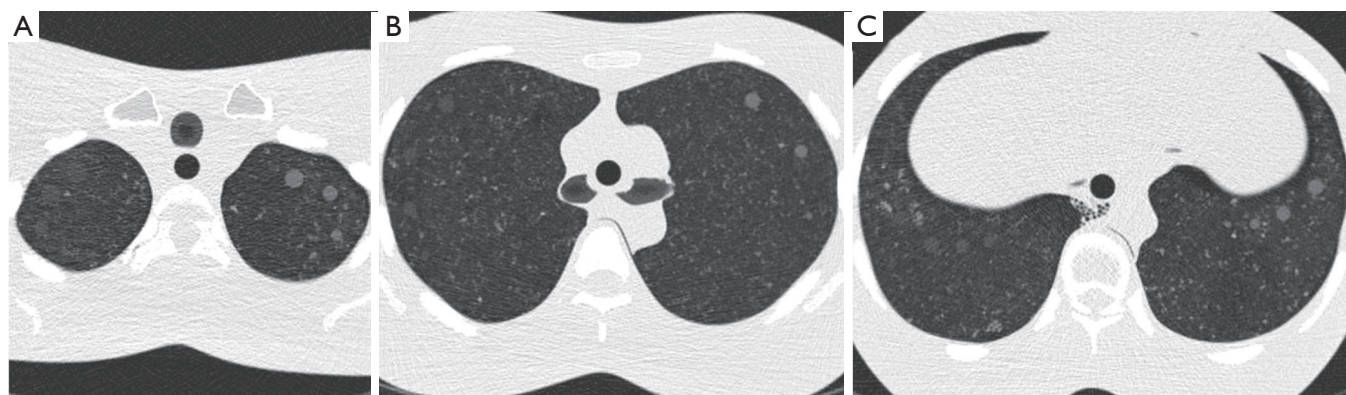
Figure 1 Anthropomorphic phantom with simulated subsolid nodules separately embedded in (A) apices, (B) bifurcation, and (C) base of lungs. The nodules in the right and left lung have 100 and 270 HU contrast to the background, respectively.

CT screening. Therefore, it is important for screening to remain effective while reducing the radiation dose; the radiation dose should not be sufficiently low to cause problems in nodule detection or measurement.

It is common to reduce the tube current to reduce the radiation dose in screening CT (5) and the use of the iterative reconstruction technique is known to reduce the radiation dose while maintaining nodule detectability (6). However, small subsolid nodules are not known to exhibit high measurement repeatability in low-dose CT (7). Recent studies, which compared the repeatability of subsolid nodule measurement with iterative reconstruction versus filtered back projection, have shown mixed results regarding whether iterative reconstruction can significantly increase measurement repeatability (7-9).

An important reason for the low repeatability of subsolid nodule measurement in low-dose CT is the presence of beam-hardening artifacts (7). Because monoenergetic images of recently used spectral CTs are effective in reducing the beam-hardening artifacts (10-12), the use of monoenergetic images may increase the measurement repeatability of subsolid nodules in low-dose CT. Therefore, our phantom study aimed to determine whether monoenergetic images captured with dual-layer spectral CT can improve the repeatability of subsolid nodule measurement and whether this approach can further reduce the radiation dose of CT while maintaining measurement repeatability.

Methods

This study was exempt from Institutional Review Board approval of Seoul National University Bundang Hospital

because no animal or human data were acquired.

Anthropomorphic phantom and simulated subsolid nodules

Lung cancer screening CT phantom (LSCT001, Kyoto Kagaku, Japan) is an anthropomorphic phantom dedicated to lung cancer screening conditions. Simulated subsolid nodules are separately embedded in apices, bifurcation, and base of lungs (*Figure 1*). We used three types of nodules in the right lung with 100 HU contrast to the background (12, 10, 8 mm), and three other types of nodules in the left lung with 270 HU contrast to the background (10, 8, 6 mm). Because six subsolid nodules were measured at three different levels, 18 measurements were obtained in one CT scan.

Image acquisition

All phantom images were obtained with two 64-row multi-detector CT machines: Brilliance 64, a conventional single-energy CT, and IQon Spectral CT (Philips Healthcare, The Netherlands). IQon Spectral CT uses a single X-ray tube and dual-layer detectors. The detectors separate the X-ray beam into low-energy (upper layer) and high-energy (lower layer) data, which are used to reconstruct spectral base images. The images contain the raw data of both layers and are used to reconstruct virtual monoenergetic images (13).

All examinations were conducted with a slice thickness of 1 mm and increment of 1 mm, with collimated detector width of 64 mm × 0.625 mm. The examinations on Brilliance 64 were performed with 120 kVp tube voltage and two distinct tube current-time products, 30 and

Table 1 Estimated radiation dose for CT protocols

Machine	Tube voltage (kVp)	Tube current-time products (mAs)	CTDI$_{vol}$ (mGy)	Radiation dose compared to typical NLST scan (%)	Radiation dose compared to proxy for NLST (%)
IQon	120	30	2.7	93	135
		15	1.4	48	70
		10	0.9	31	45
Brilliance 64	120	30	2.0	69	100
		15	1.0	34	50

CTDI, computed tomography dose index; NLST, National Lung Screening Trial.

15 mAs. The images on IQon Spectral CT were captured with 120 kVp tube voltage and three different tube current-time products: 30, 15, and 10 mAs.

Each scan from Brilliance 64 and IQon Spectral CT was repeated 30 times under the same conditions for consideration of interscan variation. Each of the images from Brilliance 64 was reconstructed by using two approaches: filtered back projection and iterative reconstruction (iDose[4] level 5, Philips Healthcare, The Netherlands), as used in our clinical routine. We reconstructed every image taken with IQon Spectral CT with a dedicated spectral iterative reconstruction algorithm (Spectral level 5, Philips Healthcare, The Netherlands) developed for the dual-layer spectral detector CT system. Virtual monoenergetic images were reconstructed from 40 to 110 keV, with 10-keV intervals on a workstation with the Spectral CT Viewer (Spectral Diagnostics Suite, Philips Healthcare, The Netherlands) (11).

Estimated radiation doses expressed in CTDIvol for all CT protocols are tabulated in *Table 1*. To calculate a proxy for the measurement repeatability in NLST (hereinafter referred to as the proxy for NLST), we used CT images that were taken at the typical NLST setting of 120 kVp tube voltage and 30 mAs tube current-time product, then reconstructed with filtered back projection (14).

Measurements

The reconstructed images were evaluated on a workstation using a commercially available computer-aided detection (CAD) system for CT examinations (IntelliSpace Portal v8, Lung Nodule Assessment, Philips Healthcare, The Netherlands). The CAD system provides quantitative information about the size of lung nodules via volume segmentation (15). It automatically performs lesion

segmentation after a user clicks on the pulmonary nodules (*Figure 2*). No manual correction was performed, except to click again when the CAD system failed on lesion segmentation. The CAD system calculated the average diameter and the volume of each lesion, according to the lesion segmentation. The average diameter is the mean of the longest diameter of the nodule and its perpendicular diameter and has been adopted in lung cancer screening guidelines (2,3).

Statistical analysis

To calculate the measurement precision of the subsolid nodules of various sizes and densities, the repeatability coefficient (RC), which solely reflects within-subject variance, was used as recommended by the Quantitative Imaging Biomarkers Alliance metrology group (16,17). The RC was presented with 95% confidence interval (CI); %RC was tabulated in the table for intuitive comprehension of measurement precision. Lower values of RC or %RC indicate better repeatability. We defined a statistically significant difference in measurement precision between the two techniques when the 95% CI ranges did not overlap. Statistical analysis was performed using commercially available software (Excel 2016, Microsoft, USA; Prism 7, GraphPad Software, USA).

Results

With the conventional single-energy CT, 30 images were taken with each of the two-tube current-time products (30 and 15 mAs) at 120 kVp tube voltage. Those images were then reconstructed by two methods of filtered back projection and iterative reconstruction (iDose[4] level 5). Therefore, 120 CT images were generated with the
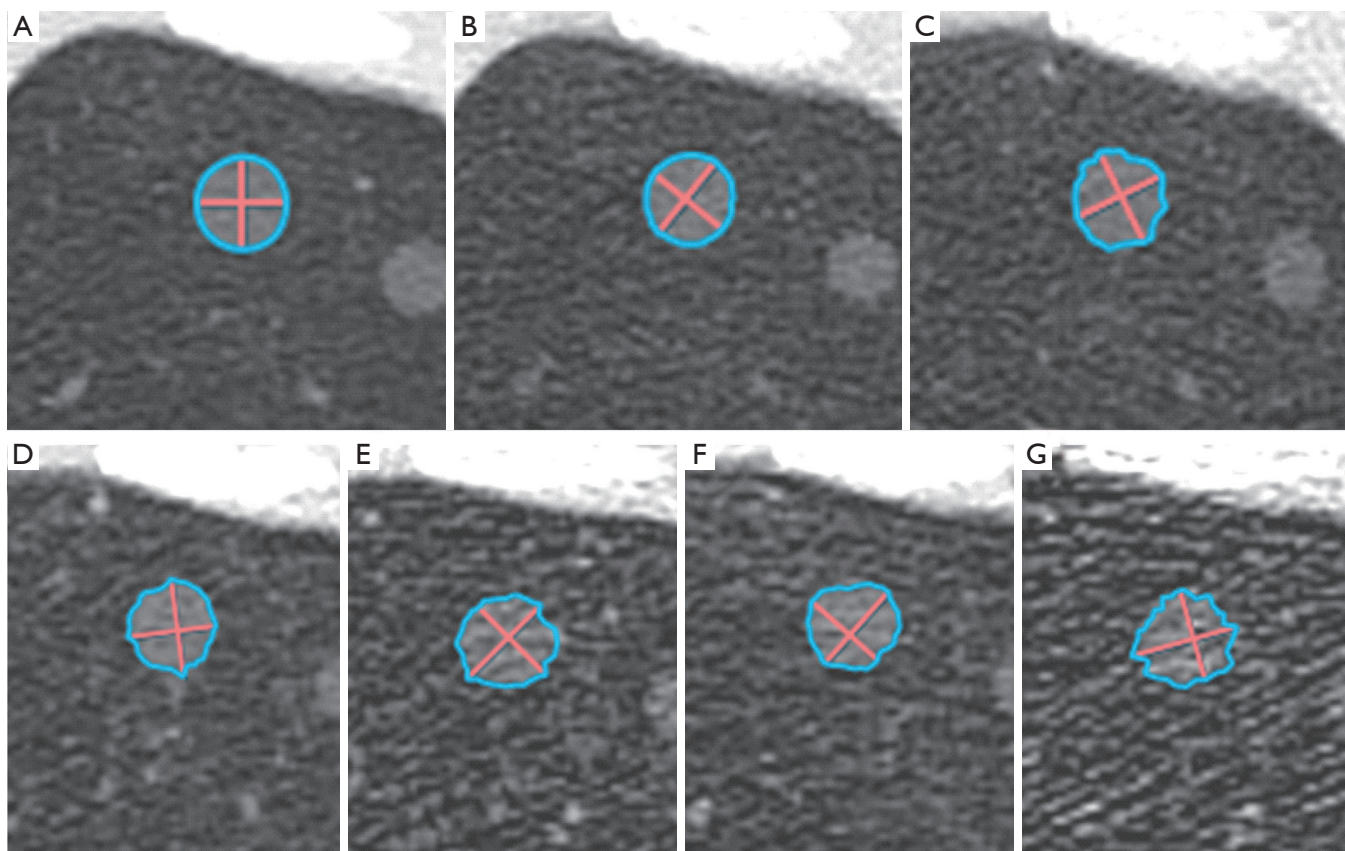
Figure 2 Automatic nodule segmentation using a computer-aided detection system for a 10 mm subsolid nodule captured with dual-layer spectral CT (A,B,C) and conventional single-energy CT (D,E,F,G). Tube current-time products and reconstruction methods of each CT protocol: (A) 30 mAs, 100 keV monoenergetic image; (B) 15 mAs, 100 keV monoenergetic image; (C) 10 mAs, 100 keV monoenergetic image; (D) 30 mAs, iterative reconstruction; (E) 30 mAs, filtered back projection; (F) 15 mAs, iterative reconstruction; and (G) 15 mAs, filtered back projection.

conventional single-energy CT. Additionally, 30 images were taken with IQon Spectral CT at the same tube voltage of 120 kVp and each of three different tube current-time products (30, 15, and 10 mAs). A total of 720 CT images were generated because we reconstructed each of the images into eight monoenergetic images at 10-keV intervals from 40 to 110 keV. With those 840 CT images, the average diameter and volume of six types of nodules were measured at three different levels of apices, bifurcation, and base of lungs. Therefore, measurement data were produced and analyzed for 15,120 nodules. The RC and %RC values for the average diameter and volume, on the basis of CT protocol and reconstruction method, are presented in *Figure 3* and *Table 2*, respectively.

The monoenergetic images taken by IQon Spectral CT showed improved measurement repeatability compared

with the images taken by the conventional single-energy CT with 120 kVp tube voltage, 30 mAs tube current-time product, and filtered back projection, which is a proxy for NLST. The RC for the average diameter and volume measurement in every set of eight monoenergetic images with 120 kVp tube voltage and 30 mAs tube current-time product was significantly lower than the proxy for NLST. The monoenergetic images with 15 mAs tube current-time product, which reduced the radiation dose by 30% relative to the proxy for NLST, also showed a lower point estimate of RC relative to the proxy for NLST. In the monoenergetic images with 10 mAs tube current-time product, the results were identical with the exception of the volume measurements at 50, 80, and 110 keV. The repeatability significantly improved in both average diameter and volume measurements in monoenergetic images of 70, 80, 100, and
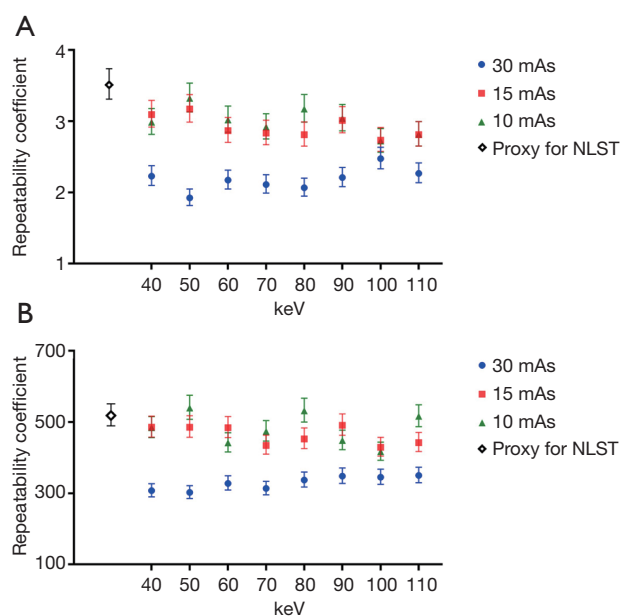
Figure 3 Repeatability coefficients of (A) average diameter and (B) volume measurements of monoenergetic images reconstructed with different energy levels, compared with the proxy for the measurement repeatability in NLST (proxy for NLST). Point estimates of repeatability coefficient are presented with 95% confidence intervals. NLST, National Lung Screening Trial.

110 keV with 15 mAs tube current-time product, as well as 60 and 100 keV with 10 mAs tube current-time product. The repeatability of average diameter measurement was significantly improved more frequently with the monoenergetic images of the reduced radiation dose (15 and 10 mAs tube current-time product), than the repeatability of volume measurement (*Figure 3*).

Table 2 shows the %RCs derived from multiple measurements of the average diameter and volume of subsolid nodules. The RC of measurements in the images of the 120 kVp tube voltage and 30 mAs tube current-time product obtained by conventional single-energy CT was lower with iterative reconstruction (iDose[4] level 5) than the RC with filtered back projection. The RC of average diameter measurement significantly improved. However, monoenergetic images taken from the same 30 mAs tube current-time product resulted in significantly lower RC than the images with iterative reconstruction. Additionally, the high energy level (60 keV or higher) monoenergetic images with reduced radiation dose of 15 mAs tube current-time product yielded a lower point estimate of RC, compared with the images with 30 mAs tube current-time

product and iterative reconstruction. The RC calculated from monoenergetic images with 10 mAs tube current-time product showed mixed results when compared with the RC from the conventional single-energy CT images with iterative reconstruction. In conventional single-energy CT, when the radiation dose was reduced by using the 15 mAs tube current-time product, the RC increased relative to the proxy for NLST. However, when iterative reconstruction was applied to the images with 15 mAs tube current-time product, measurement repeatability was comparable to that of the proxy for NLST. Of note, 100 keV monoenergetic images with 10 mAs tube current-time product showed significantly better repeatability in both average diameter and volume measurements than the images with 15 mAs tube current-time product and iterative reconstruction.

Discussion

Our study's aim was to determine whether the repeatability of subsolid nodule measurement can be controlled by using virtual monoenergetic images. In the lung cancer screening guidelines, such as lung-RADS and NCCN guideline, the average diameter is used as the size criterion for nodule follow-up and management (2,3); in the Dutch-Belgian NELSON trial, the volume was used as a similar criterion (18). Naturally, the determination of nodule follow-up and management in lung cancer screening are not based on the actual size of the nodules in surgical specimens, but on the size measured on CT and changes in size over time. Therefore, rather than focusing on the measurement accuracy of how closely the actual nodule size is measured, our study focused on the measurement precision of subsolid nodules, showing how average diameter and volume on low-dose CT were measured consistently to determine their sizes and changes.

We used calculated RC from 30 CT images from a conventional single-energy CT with a scan protocol of 120 kVp tube voltage, 30 mAs tube current-time product and filtered back projection, as a proxy for measurement repeatability in NLST. It is reasonable to assume that the measurement repeatability calculated from our proxy for NLST, which used a 64 detector-row CT machine with typical NLST protocol, is not inferior to the mean measurement repeatability of actual NLST protocols, which typically used 4- to 16-channel CT machines (14). Therefore, our results conservatively reflect the degree to which the monoenergetic image enhances measurement repeatability.

Table 2 Repeatability coefficient for subsolid nodule measurement across different tube current-time products and reconstruction methods

Tube current-time products (mAs)	Reconstruction methods	Average diameter	Volume
Brilliance 64			
30	FBP	36.4 (34.32–38.75)	117.83 (111.10–125.44)
	iDose[4]	31.97 (30.14–34.03)*	104.76 (98.78–111.53)
15	FBP	38.84 (36.62–41.35)	137.84 (129.96–146.74)**
	iDose[4]	33.76 (31.83–35.94)	112.69 (106.25–119.97)
IQon			
30	40 keV	23.93 (22.56–25.47)*	63.03 (59.43–67.10)*
	50 keV	20.13 (18.98–21.43)*	61.39 (57.88–65.35)*
	60 keV	22.71 (21.41–24.17)*	68.06 (64.17–72.46)*
	70 keV	22.12 (20.86–23.55)*	64.82 (61.12–69.01)*
	80 keV	21.64 (20.41–23.04)*	70.93 (66.88–75.51)*
	90 keV	23.12 (21.80–24.61)*	73.25 (69.07–77.99)*
	100 keV	25.75 (24.28–27.41)*	71.54 (67.45–76.16)*
	110 keV	23.81 (22.45–25.35)*	74.7 (70.43–79.53)*
15	40 keV	32.45 (30.59–34.54)	105.73 (99.69–112.56)
	50 keV	33.24 (31.34–35.38)	108.96 (102.74–116)
	60 keV	30.12 (28.40–32.06)*	104.72 (98.74–111.49)
	70 keV	29.82 (28.12–31.75)*	95.02 (89.59–101.15)*
	80 keV	29.31 (27.64–31.21)*	102.84 (96.96–109.48)*
	90 keV	31.88 (30.06–33.94)*	108.38 (102.18–115.38)
	100 keV	28.81 (27.17–30.67)*	95.05 (89.62–101.19)*
	110 keV	29.54 (27.85–31.45)*	96.65 (91.12–102.89)*
10	40 keV	31.69 (29.88–33.74)*	109.69 (103.42–116.77)
	50 keV	34.83 (32.84–37.08)	122.02 (115.04–129.9)
	60 keV	31.94 (30.11–34)*	101.61 (95.81–108.18)*
	70 keV	31.11 (29.33–33.12)*	111.25 (104.89–118.44)
	80 keV	33.59 (31.67–35.76)	126.57 (119.34–134.75)
	90 keV	32.46 (30.60–34.55)	106.14 (100.07–112.99)
	100 keV	28.94 (27.29–30.81)*	98.35 (92.73–104.70)*
	110 keV	29.89 (28.18–31.82)*	118.31 (111.55–125.95)

All CT scans were performed with a tube voltage of 120 kVp. Results are presented as %RC and 95% confidence interval in parentheses. *, significantly better than the proxy for NLST; **, significantly worse than the proxy for NLST; RC, repeatability coefficient; NLST, National Lung Screening Trial; FBP, filtered back projection.

Our study results show that monoenergetic images increase repeatability in measurement of the average diameter and volume of subsolid nodules. When compared with the proxy for NLST, the use of monoenergetic images with reduced radiation dose (tube current-time product of 50% or 33%) lowered the point estimate of the RC, which

indicated that measurement repeatability was improved, even with lower radiation risks. In monoenergetic images with tube current-time product of 15 mAs, the calculated RCs of 70, 80, 100, and 110 keV were significantly lower than the RC of the proxy for NLST, both in average diameter and volume measurement. In contrast, the RC of the volume measurement was significantly worse when the tube current-time product was reduced to 15 mAs in the conventional single-energy CT. When compared with conventional single-energy CT images using 30 mAs and iterative reconstruction (iDose[4] level 5), the point estimates of RC calculated from monoenergetic images of high energy level (60 keV or higher) were lower, even with reduced radiation dose.

Recent studies showed that monoenergetic images may improve the image quality not only by reducing beam-hardening artifacts, but also by increasing contrast-to-noise ratio (19) and reducing photon starvation artifacts (20). Even when the tube current-time product was reduced to 10 mAs, the RC of high energy level (100 keV) monoenergetic images was significantly lower than the RC of the proxy for NLST and the RC of the images with 15 mAs tube current-time product and iterative reconstruction. The significant improvements in measurement repeatability at lower radiation doses can be attributed to the reduction of beam-hardening artifacts and photon starvation artifacts.

As we measured small subsolid nodules, the %RC of volume measurement in our study was higher than that of another recent article assessing the volumetric measurement of synthetic nodules (7). This may be because of differences in the CAD system itself, or the fact that our measurement methods do not incorporate manual correction after clicking on the nodule in the CAD system. The section thickness of the CT images used in that article was 0.5 mm; whereas it was 1.0 mm in the present study. However, we believe our results are credible because we compared the RCs calculated from monoenergetic images with the proxy for NLST, which was obtained from images taken with a clinically validated CT protocol. The monoenergetic images and images with typical NLST protocol were generated and investigated in the same manner in our study. We minimized the possibility of manual intervention of investigators in our measurement methods and included a greater pool of measurement data in our study. It is understandable that the precision of volume measurement is lower for small subsolid nodules in CT images taken with a low-dose protocol when compared with an article investigating measurement reproducibility of solid pulmonary nodules (21),

Our study has limitations. First, we calculated RC with CT images of simulated subsolid nodules in an anthropomorphic phantom, rather than actual CT images of human subjects. Additional validation studies with respect to target populations may be required to apply our results to lung cancer screening. Second, it is difficult to verify the effect of different CT systems on measurement repeatability in our study. Although a recent study showed that conventional single-energy CT and dual-layer spectral CT resulted in similar image quality at equivalent dose levels (22), it is not clear whether the measurement repeatability is affected by different CT systems. However, the main purpose of our study is to determine whether monoenergetic images taken with dual-layer spectral CT have advantages over the proxy for clinically validated NLST protocol and we believe that the results of our study are in line with the purpose. Third, our study did not investigate how the measurement repeatability of the nodule is affected by the size, density, shape, or location of the nodule. However, our study design reflects our consideration of the general performance and radiation dose of the CT protocol in the detection and measurement of various lesions in a real clinical setting; notably, it does not reflect consideration of the properties of individual nodules when choosing a CT protocol for lung cancer screening. Lastly, it is not clear whether variability for subsolid nodule classification might be affected on monoenergetic images. Recent studies showed that the observer variability for subsolid nodule classification is considerable (23,24). Although another recent study showed that nodule classification exhibits interchangeability between low-dose and standard-dose chest CTs (25), further investigation is needed regarding the variability of subsolid nodule classification in monoenergetic images with lower radiation dose, as used in our study.

Conclusions

Our phantom study shows that monoenergetic images captured by using dual-layer spectral CT can improve the measurement repeatability of subsolid nodules. Therefore, the use of monoenergetic images might allow lung cancer screening with a lower radiation dose while maintaining comparable measurement repeatability.

Acknowledgements

Footnote

Conflicts of interest: The authors have no conflicts of interest to declare.

Ethical Statement: This study was exempt from Institutional Review Board approval of Seoul National University Bundang Hospital because no animal or human data were acquired.

References

1. National Lung Screening Trial Research Team, Aberle DR, Adams AM, Berg CD, Black WC, Clapp JD, Fagerstrom RM, Gareen IF, Gatsonis C, Marcus PM, Sicks JD. Reduced lung-cancer mortality with low-dose computed tomographic screening. N Engl J Med 2011;365:395-409.

2. Lung-RADS Assessment Categories, Version 1.0. American College of Radiology. Lung CT Screening Reporting and Data System (Lung-RADS™) Web site. Available online: https://www.acr.org/Clinical-Resources/Reporting-and-Data-Systems/Lung-Rads. Release date April 28, 2014. Accessed August 15, 2018.

3. Wood DE, Kazerooni EA, Baum SL, Eapen GA, Ettinger DS, Hou L, Jackman DM, Klippenstein D, Kumar R, Lackner RP, Leard LE, Lennes IT, Leung ANC, Makani SS, Massion PP, Mazzone P, Merritt RE, Meyers BF, Midthun DE, Pipavath S, Pratt C, Reddy C, Reid ME, Rotter AJ, Sachs PB, Schabath MB, Schiebler ML, Tong BC, Travis WD, Wei B, Yang SC, Gregory KM, Hughes M. Lung Cancer Screening, Version 3.2018, NCCN Clinical Practice Guidelines in Oncology. J Natl Compr Canc Netw 2018;16:412-41.

4. Brenner DJ. Radiation risks potentially associated with low-dose CT screening of adult smokers for lung cancer. Radiology 2004;231:440-5.

5. Kubo T, Lin PJ, Stiller W, Takahashi M, Kauczor HU, Ohno Y, Hatabu H. Radiation dose reduction in chest CT: a review. AJR Am J Roentgenol 2008;190:335-43.

6. Katsura M, Matsuda I, Akahane M, Yasaka K, Hanaoka S, Akai H, Sato J, Kunimatsu A, Ohtomo K. Model-based iterative reconstruction technique for ultralow-dose chest CT: comparison of pulmonary nodule detectability with the adaptive statistical iterative reconstruction technique.

Invest Radiol 2013;48:206-12.

7. Gavrielides MA, Berman BP, Supanich M, Schultz K, Li Q, Petrick N, Zeng R, Siegelman J. Quantitative assessment of nonsolid pulmonary nodule volume with computed tomography in a phantom study. Quant Imaging Med Surg 2017;7:623-35.

8. Kim H, Park CM, Chae HD, Lee SM, Goo JM. Impact of radiation dose and iterative reconstruction on pulmonary nodule measurements at chest CT: a phantom study. Diagn Interv Radiol 2015;21:459-65.

9. Kim H, Park CM, Song YS, Lee SM, Goo JM. Influence of radiation dose and iterative reconstruction algorithms for measurement accuracy and reproducibility of pulmonary nodule volumetry: A phantom study. Eur J Radiol 2014;83:848-57.

10. Kim C, Kim D, Lee KY, Kim H, Cha J, Choo JY, Cho PK. The Optimal Energy Level of Virtual Monochromatic Images From Spectral CT for Reducing Beam-Hardening Artifacts Due to Contrast Media in the Thorax. AJR Am J Roentgenol 2018;211:557-63.

11. Neuhaus V, Abdullayev N, Grosse Hokamp N, Pahn G, Kabbasch C, Mpotsaris A, Maintz D, Borggrefe J. Improvement of Image Quality in Unenhanced Dual-Layer CT of the Head Using Virtual Monoenergetic Images Compared With Polyenergetic Single-Energy CT. Invest Radiol 2017;52:470-6.

12. Wu R, Watanabe Y, Satoh K, Liao YP, Takahashi H, Tanaka H, Tomiyama N. Quantitative Comparison of Virtual Monochromatic Images of Dual Energy Computed Tomography Systems: Beam Hardening Artifact Correction and Variance in Computed Tomography Numbers: A Phantom Study. J Comput Assist Tomogr 2018;42:648-54.

13. van Hamersvelt RW, Willemink MJ, de Jong PA, Milles J, Vlassenbroek A, Schilham AMR, Leiner T. Feasibility and accuracy of dual-layer spectral detector computed tomography for quantification of gadolinium: a phantom study. Eur Radiol 2017;27:3677-86.

14. Larke FJ, Kruger RL, Cagnon CH, Flynn MJ, McNitt-Gray MM, Wu X, Judy PF, Cody DD. Estimated radiation dose associated with low-dose chest CT of average-size participants in the National Lung Screening Trial. AJR Am J Roentgenol 2011;197:1165-9.

15. den Harder AM, Willemink MJ, van Hamersvelt RW, Vonken EP, Schilham AM, Lammers JW, Luijk B, Budde RP, Leiner T, de Jong PA. Pulmonary Nodule Volumetry at Different Low Computed Tomography Radiation Dose Levels With Hybrid and Model-Based Iterative

Reconstruction: A Within Patient Analysis. J Comput Assist Tomogr 2016;40:578-83.

16. Sullivan DC, Obuchowski NA, Kessler LG, Raunig DL, Gatsonis C, Huang EP, Kondratovich M, McShane LM, Reeves AP, Barboriak DP, Guimaraes AR, Wahl RL, Group R-QMW. Metrology Standards for Quantitative Imaging Biomarkers. Radiology 2015;277:813-25.

17. Obuchowski NA, Reeves AP, Huang EP, Wang XF, Buckler AJ, Kim HJ, Barnhart HX, Jackson EF, Giger ML, Pennello G, Toledano AY, Kalpathy-Cramer J, Apanasovich TV, Kinahan PE, Myers KJ, Goldgof DB, Barboriak DP, Gillies RJ, Schwartz LH, Sullivan DC, Algorithm Comparison Working G. Quantitative imaging biomarkers: a review of statistical methods for computer algorithm comparisons. Stat Methods Med Res 2015;24:68-106.

18. Xu DM, Gietema H, de Koning H, Vernhout R, Nackaerts K, Prokop M, Weenink C, Lammers JW, Groen H, Oudkerk M, van Klaveren R. Nodule management protocol of the NELSON randomised lung cancer screening trial. Lung Cancer 2006;54:177-84.

19. Yu L, Christner JA, Leng S, Wang J, Fletcher JG, McCollough CH. Virtual monochromatic imaging in dual-source dual-energy CT: radiation dose and image quality. Med Phys 2011;38:6371-9.

20. Bamberg F, Dierks A, Nikolaou K, Reiser MF, Becker CR, Johnson TR. Metal artifact reduction by dual energy computed tomography using monoenergetic extrapolation.

21. Wormanns D, Kohl G, Klotz E, Marheine A, Beyer F, Heindel W, Diederich S. Volumetric measurements of pulmonary nodules at multi-row detector CT: in vivo reproducibility. Eur Radiol 2004;14:86-92.

22. van Ommen F, Bennink E, Vlassenbroek A, Dankbaar JW, Schilham AMR, Viergever MA, de Jong H. Image quality of conventional images of dual-layer SPECTRAL CT: A phantom study. Med Phys 2018;45:3031-42.

23. Ridge CA, Yildirim A, Boiselle PM, Franquet T, Schaefer-Prokop CM, Tack D, Gevenois PA, Bankier AA. Differentiating between Subsolid and Solid Pulmonary Nodules at CT: Inter- and Intraobserver Agreement between Experienced Thoracic Radiologists. Radiology 2016;278:888-96.

24. van Riel SJ, Sanchez CI, Bankier AA, Naidich DP, Verschakelen J, Scholten ET, de Jong PA, Jacobs C, van Rikxoort E, Peters-Bax L, Snoeren M, Prokop M, van Ginneken B, Schaefer-Prokop C. Observer Variability for Classification of Pulmonary Nodules on Low-Dose CT Images and Its Effect on Nodule Management. Radiology 2015;277:863-71.

25. Lee KH, Lee KW, Park JH, Han K, Kim J, Lee SM, Park CM. Nodule Classification on Low-Dose Unenhanced CT and Standard-Dose Enhanced CT: Inter-Protocol Agreement and Analysis of Interchangeability. Korean J Radiol 2018;19:516-25.